

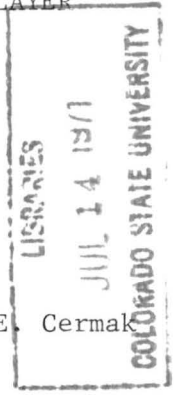
FOLIO
TA7
C6
CER-64-3
cop. 2

RECEIVED
LIBRARY
JUL 14 1964

EFFECTS OF FLEXIBLE ROUGHNESS ELEMENTS ON DIFFUSION IN A
TURBULENT BOUNDARY LAYER

BY

A. A. Quraishi and J. E. Cermak



June 1964

EFFECTS OF FLEXIBLE
ROUGHNESS ELEMENTS ON DIFFUSION IN A
TURBULENT BOUNDARY LAYER

by

A. A. Quraishi and J. E. Cornak

Paper submitted for publication to
International Journal of Air and Water Pollution

Civil Engineering Section
Colorado State University
Fort Collins, Colorado

June 1964

CER64AAQ-JEC3

LIBRARIES
COLORADO STATE UNIVERSITY
FORT COLLINS, COLORADO

MASTER FILE COPY

NOTATION

<u>Symbol</u>	<u>Definition</u>	<u>Dimension*</u>
a	Constant	----
C_{MAX}	Maximum value of concentration (ppm or mg/cc)	ML^{-3}
c	Concentration level of the diffusing matter (ppm or mg/cc)	ML^{-3}
E,F	Constants	----
$f(\sigma)$	Universal concentration function in the initial zone	----
$f(\phi)$	Universal concentration function in the intermediate zone	----
$f(\eta)$	Universal concentration function in the final zone	----
G	Flux of the diffusing matter per unit time for a unit width (ppm ft ² /sec)	$ML^{-1}T^{-1}$
h'	Height of the source (in. or cm)	L
h	Height at which the velocity is 40 percent of the ambient velocity (in.)	L
m	Constant	----
p	Exponent	----
\bar{u}_a	Mean ambient velocity (ft/sec)	LT^{-1}
\bar{u}_h	40 percent of mean ambient velocity (ft/sec)	LT^{-1}
x,y,z,	Coordinate system with origin at the beginning of the roughness, x is the longitudinal, y is the vertical, and z is the lateral distance (ft)	L
x_r	Relaxation distance (ft)	L
x'	Longitudinal distance of source from the leading edge of the roughness (ft)	L

*The symbols designating dimension have the following meaning: M = mass, T = time, L = length.

NOTATION--Cont'd

<u>Symbol</u>	<u>Definition</u>	<u>Dimension</u>
α, β	Parameter, constant, exponent or angle	----
δ	Boundary-layer thickness (in.)	L
δ_f	Boundary-layer thickness at source	L
η	$(y - h)/(\delta - h)$	----
λ	Vertical characteristic height of the diffusing plume $c(x, \lambda, 0)/C_{MAX} = 0.5$	L
σ	y/λ	----
ϕ	$(y - h)/\lambda - h$	----

EFFECTS OF FLEXIBLE
ROUGHNESS ELEMENTS ON DIFFUSION IN A
TURBULENT BOUNDARY LAYER

by

A. A. Quraishi* and J. E. Cermak**

ABSTRACT

Diffusion of ammonia gas from a line source within a turbulent boundary layer, formed by flexible roughness elements fixed on the floor of a wind-tunnel test section, was studied. The flexible roughness elements consisted of plastic strips (0.25 in. wide, 0.01 in. thick and 4 in. high) fastened to wooden strips with transverse spacing of one element per linear inch and a spacing in the direction of flow of one row every 2 in. They were arranged with their broad side facing the direction of wind. The free-stream ambient velocity was 20 ft/sec. The line source was placed at different locations and heights within the boundary layer.

The concentration field was divided into three zones according to the distance from the source and the boundary-layer thickness; an initial, an intermediate and a final zone. The experimental data were analyzed accordingly and a procedure for predicting approximate concentrations in similar cases is suggested.

The effect of source elevation was studied and it was found that as the elevation of the source was increased, the concentration at ground-level for a short distance from the source was lower than for a "ground-level" source. It increased to a peak value and then decreased asymptotically according to the law of attenuation for a source at the boundary.

* Assistant Professor, East Pakistan University of Engineering and Technology, Dacca, Pakistan.

**Professor of Engineering Mechanics, in charge of Fluid Mechanics Program, College of Engineering, Colorado State University, Fort Collins, Colorado, U.S.A.

INTRODUCTION

The question of diffusion is very important in many practical design problems and also for a better understanding of many basic problems in boundary-layer flows. Spraying of germicides and insecticides in vegetated regions, dispersion of chemical and biological particles in the lower atmosphere, evaluation of the potential danger from radio-active effluents are some of the many practical problems which require dependable quantitative estimates and sound knowledge of the fundamental processes of atmospheric diffusion under various meteorological and boundary conditions. But the difficulties encountered in evaluating, for example, the effect of various roughnesses and meteorological conditions are formidable because they are not readily expressed by a purely mathematical analysis. The K-theory and the statistical theory which were derived in the past are notable to describe the diffusion within a boundary layer. Therefore, a solution to this problem can be obtained at present only through experimentation with each group of experimental evidence contributing a small bit of information, and it is hoped that from a large number of such data the whole picture can eventually be drawn.

This paper is a summary of Quraishi's (6) work to study the spatial distributions of mean concentration in a turbulent-boundary layer formed by flexible roughness elements fixed on the floor of a wind-tunnel test section. The study was for the case of diffusion where there is no thermal stratification and matter is steadily emitted from a uniform line source placed at different positions and heights within the turbulent boundary layer. Work described in this paper is part of a systematic program to develop laboratory modeling techniques for atmospheric diffusion.

EXPERIMENTAL EQUIPMENT AND PROCEDURES

The experimental work was conducted at the Colorado State University Fluid Dynamics and Diffusion Laboratory, in a wind tunnel with a 6-ft square, 80 ft long test section. A zero pressure gradient was maintained. The test section geometry is presented schematically in Fig. 1.

The roughness consisted of strips of flexible plastic (0.25 in. wide, 0.01 in. thick and $\frac{1}{4}$ in. high) fastened to wooden strips. They were arranged to face the direction of the wind with their broad side, with transverse spacing of one element per linear inch, and a spacing in the direction of flow of one row every 2 in. The arrangement is shown in Fig. 2. All the results presented in this research were obtained at a velocity of 20 ft/sec. The velocity profiles were measured with a constant-temperature mean-velocity, hot-wire anemometer.

Anhydrous ammonia (NH_3) gas, which has a specific gravity of 0.6 compared to air, was used as the tracer gas. The gas was fed into the tunnel by two types of sources. One is $4\frac{1}{4}$ in. long line source fixed on the floor of the tunnel, 2 ft upstream from the roughness elements; the other is a 22 in. long line source whose height can be varied from 0 to 8 in. and can be located at any desired position. Cases were studied for three different locations ($x' = 8, 10$ and 12 ft) and four different source heights ($h' = 0, 2, 4$ and 8 in.) of the 22 in. long line source. The source height was varied only when the source was located at station $x' = 8$ ft. For other two locations ($x' = 10$ and 12 ft) the source was on the ground ($h' = 0$ in.). The mixture of air and ammonia gas from the tunnel was drawn through the sampling system with the help of a vacuum pump. Metered samples of air and ammonia were passed through an absorption tube containing dilute hydrochloric acid which absorbed the ammonia component of the air-ammonia mixture. The absolute quantity of ammonia gas present in each sample was determined by means of a photoelectric colorimeter which was previously calibrated. The detail of gas feed and sampling system is shown in Fig. 3.

INTERPRETATION OF EXPERIMENTAL RESULTS

Velocity Field: In order to establish the velocity field, vertical velocity profiles were taken over the roughness elements for three different velocities of 10, 20, and 40 fps at various stations downstream from the leading edge of the roughness cover. For the profiles inside the roughness cover a correlation was obtained by defining arbitrarily a velocity \bar{u}_h

which is equal to $0.4 \bar{u}_a$. This is the "theoretical velocity" at the canopy top. The level h depends on the wind speed and roughness geometry. With the reference velocity \bar{u}_a and height h , the velocity profiles became similar inside the roughness cover for all velocities and stations larger than 6 ft (in the first 6 ft the velocity field was still in the development stage) from the leading edge of the roughness cover.

The profiles above the roughness cover are similar if the velocity ratio is plotted versus the non-dimensional ratio $(y - h)/(z - h)$. The profiles obtained can be represented by a power law of the form

$$\frac{\bar{u}}{\bar{u}_a} = \left(\frac{y - h}{z - h} \right)^{1/3} \quad (1)$$

This $1/3$ power law which was found for the velocity profiles above the roughness cover agrees well with the result obtained by Bhaduri (1). Bhaduri used a fixed roughness which consisted of $1/4$ in. \times $1/4$ in. \times 6 ft wooden strips placed 3 in. apart. Several other comparisons of the velocity field above the roughness cover, displacing the height by the amount h , was made as done by Moore (4) and Bhaduri (1). Those comparisons show that the velocity profiles above the flexible roughness cover have characteristics similar to those for the fixed roughness. Table 1 shows the basic data of the velocity field and Fig. 4 shows a typical velocity profile.

Concentration Field: The results obtained for the velocity profiles in and above the roughness cover suggest the use of h as a meaningful height for separating the flow and diffusion field into an upper and a lower layer. The concentration profiles assume a constant vertical shape inside the roughness cover and are essentially unrelated to the boundary-layer diffusion above. The concentration profiles above the roughness cover have the same characteristics as the concentration profiles above a flat plate displaced by the height h . Therefore, the profiles were made dimensionless by dividing the elevations $y - h$ by $\lambda - h$ (Fig. 5), where λ is the height at which the mean concentration c has half the value of C_{max} . The profiles are separated into three different categories. This

agrees with the three zones postulated by Forch (5) from considerations of the importance of different terms of the diffusion equation. In order to separate the three zones in terms of distance from the source, a plot of λ/δ vs $\frac{x - x'}{h}$ was made as shown in Fig. 6. The three zone was termed as the initial zone, the intermediate zone and the final zone. The limit between initial and intermediate zones is $\frac{x - x'}{h} = 6$ and between intermediate and final zone is $\frac{x - x'}{h} = 26.5$.

Initial Zone: A distinction of initial-flow zone and initial-diffusion zone must be made. The velocity profiles becomes similar for all stations beyond 6 ft from the leading edge of the roughness elements. Therefore, the first 6 ft of roughness elements lie in the initial-flow zone. The initial-diffusion zone is the region for which $\frac{x - x'}{h} \leq 6$. The analysis that will follow is valid only when the source is located in the developed-flow zone. Therefore the data for the source positions $x' = 8, 10$ and 12 ft have been used in the following analysis.

The concentration profiles in this zone can be described by a dimensionless curve (Fig. 7)

$$\frac{c}{c_{\max}} = f(\sigma) \quad (2)$$

where $\sigma = y/\lambda$ and $f(1) = 0.5$. The variation of λ in this zone can be approximated by a power law of the form

$$\lambda = n (x - x')^p \quad (3)$$

The coefficients n and p can be obtained from a plot of the experimental data.

Since the concentration profiles extended very little above the height h , for this zone, it is assumed that the velocity profile follow the same law outside the height h as within the height h . This non-dimensional plot though not strictly linear is assumed to be of the linear form

$$\begin{aligned} \bar{u} &= \bar{u}_h \frac{y}{h} = \\ &= 0.4 \bar{u}_a \frac{y}{h} \end{aligned} \quad (4)$$

It now follows from the continuity equation that

$$\int_0^{\infty} c \bar{u} dy = G \quad (5)$$

where G is a constant of the diffusion field and is equal to the flux of diffusion material per unit time for a unit width of field. With Eqs. 2 and 4, Eq. 5 can be written as

$$\bar{u}_a C_{\max} = \frac{G}{0.4 \lambda^2/h \int_0^{\infty} \sigma f(\sigma) d\sigma} \quad (6)$$

The function $f(\sigma)$ has the approximate form as shown in Fig. 7. Graphical integration of $\int_0^{\infty} \sigma f(\sigma) d\sigma$ gives the value of 0.695. For an ambient velocity of 20 fps, the height h has an average value of 4.6 inches. Putting these values and substituting the value of λ from Eq. 3, Eq. 6 becomes:

$$\bar{u}_a C_{\max} = \frac{G}{0.725 \text{ m}^2 (x - x')^{2p}} \quad (7)$$

which is the equation for $\bar{u}_a C_{\max}$ in the initial zone. The dimension of \bar{u}_a is in ft/sec., C_{\max} is in parts per million. G is in ppm-ft²/sec and x is in ft.

Intermediate Zone: The expression for $\bar{u}_a C_{\max}$ for this zone can be derived from the following empirical relationships based on experimental findings.

$$1. \quad (a) \quad \frac{C}{C_{\max}} = f(\phi) \quad \text{for } y \geq h \text{ (Fig. 8)} \quad (8)$$

$$\text{where } \phi = \frac{y - h}{\lambda - h} \quad \text{and } f(1) = 0.5$$

$$(b) \quad c = C_{\max} \quad \text{for } y < h \quad (9)$$

$$2. \quad \lambda - h = a (x - x')^{\alpha} \quad (10)$$

$$3. \quad \delta - h = F x^{\beta} \quad (11)$$

$$4. (a) \frac{\bar{u}}{\bar{u}_a} = \eta^{1/n} \text{ for } h \leq y < \delta$$

$$\text{where } \eta = \frac{y-h}{\delta-h} \text{ and } n = 3 \quad (12)$$

$$(b) \bar{u} = \bar{u}_a \frac{y}{h} = 0.4 \bar{u}_a \frac{y}{h} \text{ for } y < h \quad (13)$$

$$(c) u = \bar{u}_a \text{ for } y > \delta \quad (14)$$

The continuity equation can be written in the form

$$\int_0^h c \bar{u} dy + \int_h^\infty c \bar{u} dy \quad (15)$$

With Eqs. 8, 9, 12, 13 and 14, Eq. 15 becomes:

$$\bar{u}_a C_{\max} = \frac{G}{0.2h + (\lambda - h) \left(\frac{\lambda - h}{\delta - h} \right)^{1/3} \int_0^\infty \phi^{1/3} f(\phi) d\phi} \quad (16)$$

The function $f(\phi)$ has the approximate form shown in Fig. 8. Graphical integration $\int_0^\infty \phi^{1/3} f(\phi) d\phi$ gave the value of 0.84, h for 20 fps velocity has the average value of 4.6 inches. With these values and Eqs. 10, and 11, Eq. 16 becomes:

$$\bar{u}_a C_{\max} = \frac{G}{0.077 + 0.84 \frac{e^{1.33} (x - x')^{1.33} \alpha}{F^{0.33} x^{0.33}}} \quad (17)$$

Equation 17 is the approximate form for $\bar{u}_a C_{\max}$ in the intermediate zone. The dimensions of $\bar{u}_a C_{\max}$, G and x are the same as in Eq. 7.

Final Zone: Forch (5) has shown that in this zone the velocity profiles and the concentration profiles will develop in a similar manner. The same trend may be expected for the present study. The length of the roughness elements was insufficient to establish the final zone when the source is located in the developed-flow zone. Only the last three measurements (stations 14, 16 and 18 ft) for the 44 in. long ground line source, which was located 2 ft upstream of the roughness elements seemed to fall in the final diffusion zone and have been used for the analysis of this zone.

The following empirical relationships based on experimental findings were used to find an expression of $\bar{u}_a C_{\max}$ for the final zone:

$$\frac{C}{C_{\max}} = f(\eta) \text{ for } y \geq h \text{ (Fig. 9)} \quad (18)$$

$$\text{where } \eta = \frac{y - h}{\delta - h}$$

$$C = C_{\max} \text{ for } y < h \quad (19)$$

The variations of $\delta - h$ and \bar{u} are as in Eqs. 11, 12, 13, and 14.

The continuity equation of the form as in Eq. 15 with Eqs. 16, 19, 12, 13 and 14 becomes:

$$\bar{u}_a C_{\max} = \frac{G}{0.2h + (\delta - h) \int_0^{\infty} \eta^{1/3} f(\eta) d\eta} \quad (20)$$

The function $f(\eta)$ has the approximate form as shown in Fig. 9. Graphical integration of $\int_0^{\infty} \eta^{1/3} f(\eta) d\eta$ gave the value of 0.46. For 20 fps velocity, h has the average value of 4.6 inches. With the foregoing values and Eq. 11, Eq. 20 becomes:

$$\bar{u}_a C_{\max} = \frac{G}{0.077 + 0.46 F x^{\beta}} \quad (21)$$

Equation 21 is the approximate for for $\bar{u}_a C_{\max}$ in the final zone. The dimensions of $\bar{u}_a C_{\max}$, G and x are the same as in Eqs. 7 and 17.

The agreement of $\bar{u}_a C_{\max}$ predicted by the empirical Eqs. 7, 17 and 21 with experimental results are excellent as shown in Figs. 10, 11, 12, and 13.

Effect of Source Elevation: The effect of source elevation is shown in Fig. 14. The plot follows a similar trend as found by Davar (3), only the slope is different in both cases. This is expected because of the difference in roughness.

As the elevation of the source is increased, the ground-level concentration for a short distance from the source is lower than for a "ground-level" source. They rise to a peak value and then decrease asymptotically according to the law of attenuation for a source at the

boundary. The distance that must be traversed before the concentrations follow the law of attenuation for a source at the boundary is termed a relaxation distance and denoted by x_r . This relaxation distance is plotted against h'/δ_1 in Fig. 15. It is found that it follows a power law of the form

$$x_r = E \frac{h'}{\delta_1} \quad (22)$$

where E is a constant h' is the source height, and δ_1 is the boundary layer thickness at the location of the source. In this experiment the constant E has the value of 10. In the same figure data from Davar (3) was also plotted and was found to follow the same law with constant E equal to 13.

Significance of Results: Atmospheric diffusion of great practical consequences e.g. over crops and forests occur in the air layer adjacent to the earth's surface; flow conditions in this layer can be closely simulated in a wind tunnel by the inner portion of a boundary layer generated by air flows over simulated crops or a forest.

Cermak (2) has made a comparison of wind tunnel data and some field data while developing a Lagrangian similarity hypothesis for modeling diffusion in turbulent shear flow. The similarity hypothesis shows good agreement between wind-tunnel and field data.

CONCLUSIONS

As a result of this study of diffusion from a line source in a turbulent boundary layer formed by the flexible roughness elements fixed on the floor of the wind tunnel test section, the following main conclusions can be drawn:

(1) Separation of the diffusion field into three zones namely, initial, intermediate and final zone, simplifies the description of the diffusion process. The limits of the three zones are described by the parameter $(x - x')/h$. The intermediate zone is between the limit $6 < (x - x')/h < 26.5$. When the ratio $(x - x')/h$ is less than 6 and greater than 46.5 the initial and final zones respectively are found.

The maximum concentration for the three zones can be approximated by Eqs. 7, 17, and 21.

(2) The concentration profiles assume a constant vertical shape inside the roughness cover and are essentially unrelated to the boundary-layer diffusion above. The vertical concentration distribution above the roughness cover for the three zones can be approximated by dimensionless universal curves (Eqs. 2, 6, and 16 and shown in Figs. 7, 8, and 9), and have essentially the same characteristics as the concentration profiles above a flat plate displaced by the height h .

(3) For an elevated source, the relaxation distance, which has been defined as the distance that must be traversed before the concentration follows the law of attenuation for a source at the boundary, has been found to be of the form:

$$x_1 = E \frac{h'}{\delta_f}$$

ACKNOWLEDGEMENTS

Sponsorship for this study was provided by the Agricultural Research Service under Contract No. 12-14-100-4546(41) and the U.S. Army Electronic Research and Development Activity, Fort Huachuca, Arizona under Grant No. DA-SIG-36-039-62-024.

REFERENCES

1. Bhaduri, S. Mass Diffusion from a Point Source in a Turbulent Boundary Layer Over a Rough Surface. Ph.D. Dissertation, Colorado State University, Fort Collins, Colorado, July 1963, 167 p.
2. Cermak, J. E. Lagrangian Similarity Hypothesis Applied to Diffusion in Turbulent Shear Flow. Journal of Fluid Mechanics, Vol. 15, Part I, pp. 49-64, 1963.
3. Davaar, K. S. Diffusion from a Point Source within a Turbulent Boundary Layer. Ph.D. Dissertation, Colorado State University, Fort Collins, Colorado, July 1961, 161 p.
4. Moore, W. L. An Experimental Investigation of the Boundary Layer Development Along a Rough Surface. Ph.D. Dissertation, Department of Mechanics and Hydraulics, State University of Iowa, Iowa City, Iowa, August 1951, 58 p.
5. Poreh, M. Diffusion from a Line Source in a Turbulent Boundary Layer. Ph.D. Dissertation, Colorado State University, Fort Collins, Colorado, 1961, 110 p.
6. Quraishi, A. A. Effects of Flexible Roughness Elements on Diffusion in a Turbulent Boundary Layer. Ph.D. Dissertation, Colorado State University, Fort Collins, Colorado, December 1963, 190 p.

TABLE I.--BASIC DATA (VELOCITY FIELD)

x ft.	\bar{u}_x ft./sec.	b in.	θ in.	u_x^* ft./sec.	h in.	Average h in.
2	10	10.5	--	--	5.2	5.7
6	"	16.0	--	--	6.3	"
10	"	16.0	--	--	5.5	"
12	"	17.3	--	--	5.8	"
14	"	18.7	--	--	6.3	"
16	"	20.1	--	--	4.7	"
18	"	21.5	--	--	6.2	"
2	20	9.2	--	--	4.3	4.6
6	"	11.9	1.0	2.2	5.3	"
10	"	14.6	1.52	2.05	4.2	"
12	"	16.0	1.76	2.0	4.5	"
14	"	17.3	1.99	1.9	4.8	"
16	"	18.6	2.21	1.84	4.7	"
18	"	20.0	2.41	1.84	4.6	"
2	40	8.6	--	--	2.3	3.8
6	"	10.9	--	--	4.2	"
10	"	13.3	--	--	3.8	"
12	"	14.3	--	--	3.6	"
14	"	15.6	--	--	3.9	"
16	"	16.7	--	--	4.3	"
18	"	17.9	--	--	4.0	"